Perturbed $5snd\ ^{1,3}D_2$ Rydberg series of Sr

C. J. Dai
Department of Physics, Zhejiang University, Hangzhou 310027, People's Republic of China
(Received 23 January 1995; revised manuscript received 19 June 1995)

The energy levels of the Sr $5snd\ ^{1,3}D_2$ Rydberg series have been measured using an autoionization scheme, which provides an excellent opportunity for the application of the multichannel quantum-defect theory (MQDT) to their spectra. MQDT parametrizations of the $^{1,3}D_2$ bound-state Rydberg series are presented, including calculated term values for these series. Furthermore, it is found that MQDT wave functions that are derived from experimentally determined level energies are capable of predicting such wave-function-sensitive properties as natural radiative lifetimes of Sr $5snd\ ^{1,3}D_2$ Rydberg states.

PACS number(s): 32.70.Fw, 32.70.Jz, 31.50.+ w

I. INTRODUCTION

A considerable number of experiments to investigate the Rydberg-state structure of the Sr atom has been performed in the last two decades. Meanwhile, multichannel quantum-defect theory (MQDT) has evolved into a powerful tool for the interpretation of these atomic data [1–5]. MQDT wave functions that were derived from the measured energies of the Rydberg states were successfully used to predict the g_J factors [6], the hyperfine structure [7], and other observables. A theoretical investigation was devoted to radiative lifetimes of the low-lying states ($n \leqslant 9$) recently [8]. Lifetimes of Sr $5snd\ ^{1,3}D_2$ states have been measured by several groups [9,10]. However, to our knowledge, the theoretical interpretation for those states with $n \geqslant 10$ has not yet been performed.

In this work, we report the measurement of energy levels of the Sr $5snd\ ^{1,3}D_2$ series with a different detection scheme, whose data are analyzed with MQDT parametrizations. The parameters that are yielded are used to calculate energies and wave functions, followed by an explicit application of the MQDT to the prediction of natural radiative lifetimes of the Rydberg states.

The energy levels of Sr $5snd$ Rydberg states have been measured by several groups using various detection methods [1–4]. In this paper a different detection scheme is used to measure Sr $5snd\ ^{1,3}D_2$ Rydberg series, i.e., Rydberg atoms are detected by measuring the ions produced via an autoionization process. As we know, the autoionization process has attracted much attention of scientists since it has many advantages over the direct photoionization. It can serve many purposes, such as laser isotope separation [11], development of new lasers [12], and dielectronic recombination [13]. More recently it was listed as an important candidate for lasing without population inversion [14]. Here we demonstrate another application—detection of Rydberg atoms.

However, interactions in Rydberg series have been given new impetus by extensive studies. The radiative lifetime of a Rydberg state, among other things, is a good candidate for such purposes. Lifetime is sensitive to perturbation by doubly excited states because of the great difference in lifetimes between the Rydberg states (long lived) and the low-lying valence perturber states (short lived). The wave functions obtained from MQDT treatments of our data are tested by lifetime calculations. It is of considerable interest to check to what extent the MQDT wave function can be used for a reliable prediction of lifetimes.

II. EXPERIMENTAL METHODS

Three dye lasers are pumped by the same neodymium-doped yttrium aluminum garnet (Nd: YAG) pulsed laser in the experiment. In order to generate photons whose wavelengths match the excitation scheme shown in Fig. 1, the third-harmonic generation of the pumping laser in used. The experimental configuration is diagrammed in Fig. 2 following the conventional setup for the three-step spectroscopy. In the first two steps the photons at wavelengths of λ_1 and λ_2 excite Sr atoms in an atomic beam from the $5s^2$ state to the

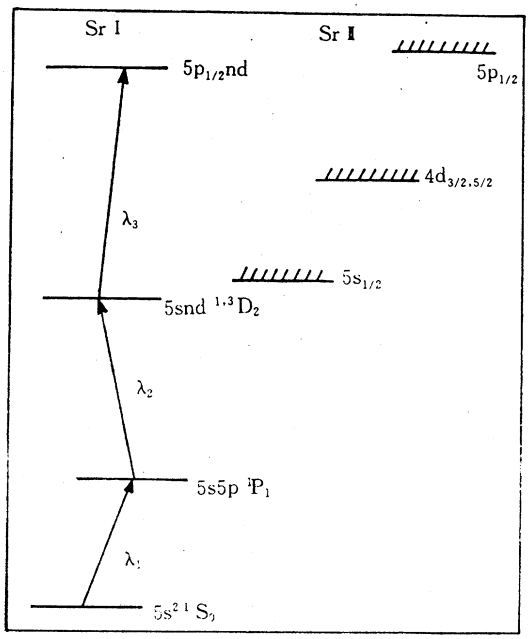

FIG. 1. Excitation scheme for the Sr autoionizing states. The first laser is fixed at 460.9 nm; the third laser is fixed near the resonance line of Sr II, which is $5s_{1/2}$—$5p_{1/2}$ at 421.7 nm. The second laser is tuned to excite many $5snd$ Rydberg states.

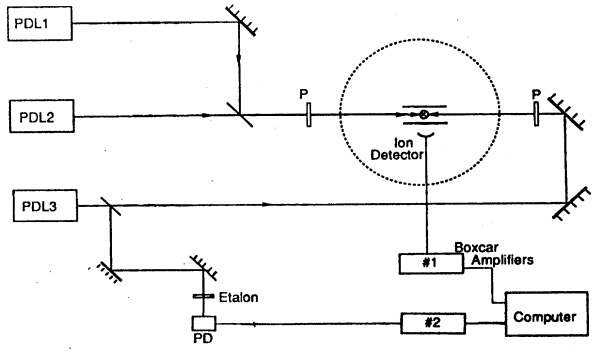

FIG. 2. Experimental configuration. Three dye lasers are pumped by the third harmonics of the Nd: YAG pulsed laser. The atomic beam is made inside a vacuum chamber where the three-step excitation is performed. The ions produced are detected by a channeltron and averaged by a boxcar, from which the final signals are recorded in a computer via an ADC converter. A Fabry-Perot étalon with a photoiode is used to calibrate the photon energy.

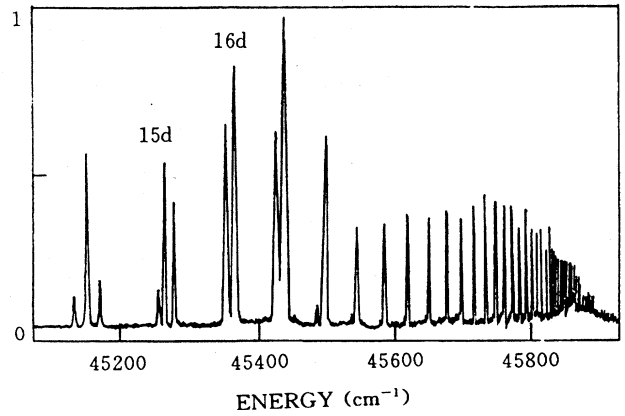

FIG. 3. Example of the measured spectra of the $5snd\ ^{1,3}D_2$ Rydberg series. The higher energy peak in each pair starts to be the more intense peak at $n=16$, indicating that the two series exchange their characters.

$5s5p$ state, and then to the $5snd$ Rydberg states. After a time delay of 0.5 μs, a third laser at a wavelength of 421.7 nm is fired to excite the remaining $5s$ electron, resulting in an autoionizing $5p_{1/2}nd$ state. After another 0.5 μs we apply a modest electric field to sweep the ions produced by autoionization into a channeltron detector. The excitation scheme described is the so-called isolated core excitation [15]. It has several very appealing features, and has been used extensively for studying autoionization spectra [16].

The photons interact with Sr atoms in a vacuum chamber, where the atomic beam is made by a heating system. The atomic beam is collimated and perpendicular to the laser beams to reduce the Doppler broadening. The wavelength of photon driving the $5s^2 \rightarrow 5s5p$ transition is fixed at 460.9 nm, while the one for the $5s5p \rightarrow 5snd$ transition is tuned to populate different n states. The third laser drives Rydberg atoms to autoionizing states, whose wavelength is slightly shifted from the ion resonance line. The shift depends on the difference in the quantum defects of the $5snd$ and $5p_{1/2}nd$ states. The $5p_{1/2}nd$ states have quantum defects that are 0.55 greater than those of the $5snd\ ^1D_2$ states.

The polarization of dye lasers is controlled by polarizers to ensure a high degree of linear polarization, which enables us to excite both $J=0$ and 2 states with the first two lasers. The $J=2$ states can be easily identified in a spectrum, from which many members of Sr $5snd\ ^1D_2$ ($9 \leqslant n \leqslant 50$) and $5snd\ ^3D_2$ series ($9 \leqslant n \leqslant 37$) have been determined. Due to the singlet-triplet mixing caused by the spin-orbit interaction around $n=16$, transitions to $5snd\ ^3D_2$ states become allowed from the $5s5p\ ^1P_1$ state, although they usually have a weaker intensity in the spectrum of $J=2$ states. A typical scan of the second laser's wavelength is shown in Fig. 3, which demonstrates the exchange of the character between the singlet and triplet states at $n=16$ (the higher-energy peak in each pair starts to become the more intense one).

The linewidth of lasers is better than 0.5 cm^{-1} to ensure a reasonable resolution. To calibrate a spectrum, a beam splitter introduces a beam from the second laser to pass through an F-P étalon, whose interference signals are recorded with a photodiode. The absolute calibration for the second laser is done using the two well-known frequency marker lines [17]. The second laser provides photons at wavelengths of 421.3 and 422.6 nm, making transitions from $5s5p\ ^1P_1$ states to the $5s16d$ and $5s17d$ states and subsequently to the autoionizing $5p_{1/2}16d$ and $5p_{1/2}17d$ states, so that the first two lasers alone produce a large ionization signal. The ionization signal outputed from the detector is amplified and averaged by a boxcar, and stored in a computer via an analog-to-digital converter for further analysis.

The experimental energies from the present experiment and previous ones (states with $n<9$ are taken from Ref. [18]; states with $n>50$ are cited from Ref. [2]) are listed in Table I for $5snd\ ^1D_2$ and Table II for $5snd\ ^3D_2$ sequences, respectively. The typical uncertainty of the experiment is estimated to be 0.2 cm^{-1}. The corresponding MQDT calculated values are also tabulated for handy comparison. The MQDT calculations involved will be detailed in the following sections.

It is worthwhile to point out that our data show general agreement with that of Ref. [1] within their uncertainties (see Tables I and II). In Ref. [1], the experiment was conducted in a heated pipe using multiphonon ionization spectroscopy. It is evident that the signal-to-noise ratio is significantly improved in this work.

III. THEORY

A great variety of atomic data, such as spectrum [19–21], photoelectron angular distribution [22–24], etc., has been successfully interpreted using the MQDT as a tool. The MQDT was first formulated by Seaton [25], and has been further developed by several groups [26]. It has been successfully used to reproduce the complex features of the multielectron atoms and of a few molecules. Since MQDT analysis of complex spectra is a well-documented procedure, only some basic principles of it are described here.

According to the MQDT, energy levels of a Rydberg series are simultaneous solutions of the following equations:

$$E = I_i - R/\nu_i^2 \tag{1}$$

TABLE I. Energy Levels of Sr $5snd\ ^1D_2$ Rydberg States. The data with $n=6-8$ and $n=51-84$ are from Refs. [18] and [2], respectively. The rest of the data are from the present experiment, whose typical error is about 0.2 cm^{-1}. The theoretical values are from the three-channel MQDT calculations. The present results are compared with the previous work of Esherick [1].

	Present				Previous [1]			
	Expt.		Calc.		Expt.		Calc.	
n	E (cm^{-1})	n^*	E (cm^{-1})	n^*	E (cm^{-1})	n^*	E (cm^{-1})	n^*
6	39 733.11	4.207	39 734.05	4.208	39 733.11	4.207	39 736.04	4.208
7	41 831.70	5.173	41 831.03	5.173	41 831.70	5.173	41 828.83	5.171
8	43 020.90	6.139	43 019.33	6.138	43 020.90	6.139	43 019.69	6.138
9	43 755.98	7.101	43 755.49	7.100	43 755.88	7.101	43 755.74	7.101
10	44 241.86	8.057	44 242.78	8.059	44 241.70	8.057	44 242.39	8.059
11	44 578.62	9.004	44 582.15	9.016	44 578.58	9.004	44 581.33	9.013
12	44 829.47	9.976	44 828.08	9.969	44 829.40	9.975	44 827.26	9.966
13	45 011.81	10.919	45 011.72	10.919	45 011.77	10.919	45 011.57	10.918
14	45 153.03	11.868	45 150.15	11.846	45 153.10	11.868	45 153.14	11.868
15	45 263.62	12.811	45 230.05	12.501	45 263.62	12.811	45 263.57	12.811
16	45 362.17	13.875	45 362.20	13.875	45 362.03	13.873	45 361.98	13.872
17	45 433.26	14.830	45 422.50	14.834	45 433.14	14.829	45 433.16	14.829
18	45 492.74	15.802	45 492.88	15.805	45 492.48	15.797	45 492.53	15.798
19	45 452.36	16.778	45 542.54	16.782	45 542.12	16.773	45 542.24	16.775
20	45 584.23	17.758	45 584.38	17.762	45 584.17	17.757	45 584.15	17.756
21	45 619.63	18.737	45 619.92	18.746	45 619.60	18.736	45 619.76	18.741
22	45 650.27	19.729	45 650.36	19.732	45 650.26	19.729	45 650.24	19.728
23	45 676.49	20.716	45 676.62	20.721	45 676.51	20.717	45 676.52	20.717
24	45 699.31	21.707	45 699.38	21.710	45 699.25	21.704	45 699.32	21.707
25	45 719.16	22.696	45 719.28	22.702	45 719.25	22.701	45 719.23	22.700
26	45 736.83	23.700	45 736.74	23.694	45 736.80	23.698	45 736.71	23.693
27	45 752.24	24.694	45 752.15	24.688	45 752.22	24.692	45 752.13	24.686
28	45 765.77	25.678	45 765.82	25.682	45 765.79	25.679	45 765.81	25.681
29	45 778.02	26.679	45 778.00	26.677	45 777.97	26.674	45 777.99	26.676
30	45 788.92	27.675	45 788.89	27.672	45 788.90	27.673	45 788.89	27.672
31	45 798.69	28.669	45 798.67	28.667	45 798.65	28.665	45 798.78	28.679
32	45 807.43	29.657	45 807.49	29.664	45 807.46	29.660	45 807.50	29.665
33	45 815.53	30.669	45 815.47	30.661	45 815.60	30.678	45 815.47	30.661
34	45 822.51	31.629	45 822.71	31.658	45 822.71	31.658	45 822.71	31.658
35	45 829.34	32.663	45 829.29	32.665	45 829.32	32.660	45 829.30	32.656
36	45 835.36	33.663	45 835.30	33.652	45 835.30	33.652	45 835.31	33.654
37	45 840.43	34.580	45 840.80	34.650	45 840.85	34.659	45 840.81	34.652
38	45 845.73	35.624	45 845.85	35.649	45 845.91	35.661	45 845.85	35.649
39	45 850.54	36.658	45 950.49	36.647	45 850.53	36.656	45 850.49	36.647
40	45 854.81	37.656	45 854.76	37.644	45 854.83	37.661	45 854.77	37.646
41	45 858.76	38.655	45 858.71	38.642	45 858.75	38.653	45 858.72	38.645
42	45 862.41	39.653	45 862.37	39.642	45 862.44	39.662	45 862.37	39.642
43	45 865.81	40.656	45 865.76	40.641	45 865.84	40.665	45 865.76	40.641
44	45 868.99	41.666	45 868.92	41.640	45 868.99	41.666	45 868.91	41.640
45	45 871.94	42.674	45 871.84	42.638	45 871.91	42.663	45 871.84	42.638
46	45 874.61	43.652	45 874.57	43.637	45 874.61	43.652	45 874.57	43.637
47	45 877.16	44.652	45 877.12	44.635	45 877.10	44.627	45 877.12	44.635
48	45 879.56	45.658	45 879.50	45.632	45 879.51	45.636	45 879.50	45.632
49	45 881.82	46.671	45 881.74	46.634	45 881.76	46.643	45 881.74	46.634
50	45 833.86	47.646	45 883.83	47.631	45 883.83	47.631	45 883.83	47.631
51	45 885.80	48.631	45 885.80	48.631	45 885.75	48.605	45 885.80	48.631
52	45 887.61	49.609	45 887.60	49.603	45 887.61	49.609	45 887.65	49.631
53	45 889.38	50.624	45 889.34	50.600	45 889.38	50.624	45 889.39	50.629
54	45 891.03	51.628	45 890.99	51.603	45 891.03	51.628	45 891.03	51.628
55	45 892.59	52.635	45 892.54	52.602	45 892.59	52.635	45 892.58	52.628

TABLE I. (*Continued*).

	Present				Previous [1]			
	Expt.		Calc.		Expt.		Calc.	
n	E (cm^{-1})	n^*	E (cm^{-1})	n^*	E (cm^{-1})	n^*	E (cm^{-1})	n^*
56	45 894.04	53.626	45 894.00	53.597	45 894.04	53.626	45 894.04	53.626
57	45 895.39	54.600	45 895.39	54.600	45 895.39	54.600	45 895.42	54.622
58	45 896.74	55.630	45 896.70	55.598	45 896.74	55.630	45 896.73	55.622
59	45 898.01	56.653	45 897.95	56.604	45 898.01	56.653	45 897.97	56.620
60	45 899.20	57.666	45 899.12	57.596	45 899.20	57.666	45 899.15	57.622
61	45 900.27	58.624	45 900.24	58.597			45 900.27	58.624
62	45 901.33	59.622	45 901.30	59.593			45 901.33	59.622
63	45 902.34	60.622	45 902.32	60.602			45 902.34	60.622
64	45 903.30	61.621	45 903.28	61.599			45 903.30	61.621
65	45 904.22	62.626	45 904.20	62.603			45 904.21	62.614
66	45 905.09	63.623	45 905.07	63.599			45 905.08	63.611
67	45 905.92	64.619	45 905.90	64.595			45 905.92	64.619
68	45 906.72	65.626	45 906.70	65.600			45 906.71	65.613
69	45 907.48	66.627	45 907.46	66.600			45 907.47	66.614
70	45 908.19	67.605	45 908.18	67.591			45 908.19	67.605
71			45 908.88	68.598				
72			45 909.54	69.590				
73			45 910.18	70.594				
74	45 910.81	71.626	45 910.79	71.592				
75	45 911.39	72.617	45 911.38	72.600				
76			45 911.94	73.596				
77			45 912.48	74.597				
78			45 913.00	75.601				
79	45 913.50	76.605	45 913.49	76.584				
80	45 913.98	77.607	45 913.97	77.586				
81			45 914.43	78.584				
82			45 914.88	79.598				
83			45 915.30	80.581				
84	45 915.72	81.601	45 915.71	81.577				
85			45 916.11	82.584				

and

$$\det|F_{i\alpha}| = \det|U_{i\alpha}\sin[\pi(\nu_i+\mu_\alpha)]| = 0, \tag{2}$$

where R is the mass-corrected Rydberg constant and I_i is the ionization limit corresponding to the state of ion core in the ith collision channel; ν_i is the effective quantum number relative to the I_i ionization limit, and μ_α is the eigenchannel quantum defect; $U_{i\alpha}$ is the element of a unitary frame transformation, U, between the i collision channels and the α eigenchannels, which describes the long-range Coulomb interactions and the short-range effects of the many-electron interactions, respectively. An analysis of a spectrum thus consists of adjusting the μ_α and $U_{i\alpha}$ so that the term values given by Eqs. (1) and (2) agree with the experimental data. In addition to providing a means of fitting experimentally determined eigenstate energies, the MQDT also constructs the normalized wave functions for the highly excited state ψ, which may be expressed either as a superposition of the i collision channels

$$\psi = \sum_i A_i \varphi_i \tag{3}$$

or as a linear combination of the α channels

$$\psi = \sum_\alpha B_\alpha \psi_\alpha, \tag{4}$$

where the B_α are the coefficients of the eigenfunction in the ψ_α basis, which are determined by Eq. (2) via the cofactors of $\det|F_{i\alpha}|$ as

$$B_\alpha = \mathrm{cof}(i,\alpha) \Big/ \left[\sum_\alpha \mathrm{cof}^2(i,\alpha)\right]^{1/2}, \tag{5}$$

which yields the mixing coefficients $A_i^{(n)}$ of the ith collision channel in the nth eigenstate, i.e.,

$$A_i^{(n)} = (-1)^{(l_i+1)}\nu_i^{3/2}\Sigma_\alpha U_{i\alpha}\cos[\pi(\nu_i+\mu_\alpha)]\times B_\alpha^{(n)}/N_n, \tag{6}$$

where N_n is a normalization factor [25].

TABLE II. Energy Levels of Sr $5snd\ ^3D_2$ Rydberg States. The experimental values for $n=7-8$ states are from Ref. [18]. The rest of data are from the present experiment, whose typical error is about 0.2 cm^{-1}. The theoretical values are from the two-channel MQDT calculations. The present results are compared with the previous work by Esherick [1].

	Present				Previous [1]			
	Expt.		Calc.		Expt.		Calc.	
n	E (cm^{-1})	n^*	E (cm^{-1})	n^*	E (cm^{-1})	n^*	E (cm^{-1})	n^*
7	41 869.32	5.197	41 876.00	5.201	41 869.32	5.197	41 867.66	5.196
8	43 070.31	6.192	43 069.16	6.191	43 070.311	6.192	43 070.16	6.192
9	43 804.69	7.182	43 802.54	7.178	43 804.89	7.182	43 805.33	7.183
10	44 286.91	8.167	44 284.86	8.162	44 287.05	8.167	44 287.54	8.168
11	44 619.84	9.144	44 618.47	9.140	44 620.08	9.145	44 620.59	9.147
12	44 859.31	10.113	44 858.29	10.109	44 860.28	10.118	44 859.82	10.116
13	45 036.52	11.069	45 035.85	11.065	45 036.85	11.071	45 036.93	11.071
14	45 171.43	12.010	45 170.31	12.001	45 171.54	12.011	45 171.40	12.010
15	45 276.45	12.936	45 274.14	12.913	45 276.62	12.938	45 276.49	12.937
16	45 350.57	13.736	45 356.40	13.805	45 350.35	13.733	45 350.47	13.735
17	45 421.04	14.652	45 424.04	14.695	45 420.78	14.648	45 420.80	14.649
18	45 479.92	15.577	45 481.51	15.604	45 479.88	15.576	45 481.87	15.610
19	45 530.53	16.529	45 530.95	16.537	45 530.17	16.521	45 530.21	16.522
20			45 573.51	17.491			45 573.23	17.484
21			45 610.12	18.458			45 610.08	18.457
22	45 641.69	19.435	45 641.67	19.435	45 641.68	19.435	45 641.75	19.437
23	45 669.09	20.422	45 668.96	20.417	45 669.14	20.424	45 669.09	20.422
24	45 692.84	21.412	45 692.67	21.404	45 692.81	21.410	45 692.82	21.411
25	45 713.48	22.399	45 713.37	22.394	45 713.51	22.401	45 713.53	22.402
26	45 731.76	23.398	45 731.54	23.385	45 731.80	23.401	45 731.69	23.394
27	45 747.71	24.389	45 747.55	24.378	45 747.81	24.395	45 747.70	24.388
28			45,761.74	25.373			45 761.88	25.383
29	45 774.56	26.384	45 774.37	26.368	45 774.58	26.386	45 774.50	26.379
30	45 785.81	27.379	45 785.65	27.364	45 785.87	27.385	45 785.77	27.375
31	45 795.94	28.379	45 795.76	28.360	45 795.91	28.376	45 795.88	28.372
32	45 804.97	29.368	45 804.87	29.357	45 805.02	29.374	45 804.98	29.370
33	45 813.16	30.362	45 813.10	30.354	45 813.18	30.364	45 813.20	30.367
34	45 820.71	31.373	45 820.56	31.352	45 820.69	31.370	45 820.65	31.365
35	45 827.53	32.379	45 827.34	32.350	45 827.55	32.382	45 827.42	32.362
36	45 833.56	33.354	45 833.53	33.349	45 833.54	33.351	45 833.60	33.361
37	45 839.34	34.376	45 839.18	34.347	45 839.32	34.373	45 839.25	34.360
38			45 844.36	35.345			45 844.42	35.357
39			45 849.12	36.344			45 849.18	36.357
40			45 853.51	37.344			45 853.56	37.355

The MQDT wave function should be valuable in predicting other observables such as Lande factors, natural lifetimes, Stark splittings, and hyperfine structures. However, it is worthwhile to note that different observables are sensitive to different properties of the wave functions. Here we choose to test the wave functions obtained from level energies by evaluating the natural radiative lifetimes of Sr $5snd\ ^{1,3}D_2$ Rydberg states. Since lifetime is mainly determined by the outer parts of the wave functions and is sensitive to small admixture of short-lived valence states (perturbers) into long-lived Rydberg states, it serves as a good candidate for checking wave function and reflecting configuration mixing. The analogous studies have been performed in the perturbed $6snd\ ^{1,3}D_2$ series of Ba [27] and more recently in Yb [28]. To the contrary, the MQDT analysis of lifetime data of Sr $5snd\ ^{1,3}D_2$ Rydberg states [9,10] has not yet been done, although the comparison between *ab initio* calculations with lifetime data for $n\leq 9$ was given recently [8].

The total radiative decay rate of the nth level can be expressed as

$$\Gamma_n=\Sigma_{i,j}A_i^{(n)}A_j^{(n)}\Gamma_{ij}^{(n)}, \tag{7}$$

where $A_i^{(n)}$ or $A_j^{(n)}$ is defined in Eq. (6), whereas $\Gamma_{ij}^{(n)}$ may be approximated as [28]

$$\Gamma_{ij}^{(n)}=[\nu_i^{(n)}\nu_j^{(n)}]^k\Gamma_{ij}. \tag{8}$$

This is true based on the assumption that the energy dependence of $\Gamma_{ij}^{(n)}$ can be separated from its channel dependence.

Explicitly, the adjustable parameters k and Γ_{ij} are energy independent. $\nu_i^{(n)}$ or $\nu_j^{(n)}$ is defined in Eqs. (1) and (2). The physical significance of Eq. (7) is obvious: the direct term $[A_i^{(n)}]^2\Gamma_{ii}^{(n)}$ represents the decay rate of the atom in the nth level, making spontaneous transitions to all possible lower levels through the ith channel; the cross term $A_j^{(n)}A_j^{(n)}\Gamma_{ij}$ $(i\neq j)$ means the mixing decay rate owing to the interaction between the i channels. The natural radiative lifetime of the atom in the nth excited state is then related to Eq. (7) by the following expression:

$$\tau_n = 1/\Gamma_n \ . \tag{9}$$

Armed with the theory described, we are in a position to apply it to the Sr $5snd\ ^{1,3}D_2$ Rydberg series. To do this one has to specify the MQDT model, which is supposed to be the simplest and, at the same time, sufficient to take into account most of the features in the spectra.

IV. RESULTS AND DISCUSSION

A breakdown of the strict LS-coupling scheme is pronounced for highly excited $5snd\ ^{1,3}D_2$ levels, which is the most evident near $n=15$ [1]. However, numerous studies [29] have shown that, with regard to the behavior of even-parity m_0snd, $J=2$ spectra ($m_0=4-6$ for Ca, Sr, and Ba, respectively), the spin-orbit singlet-triplet mixing is quite negligible in both Ca and Sr, whereas the same is not true for Ba. This was demonstrated by calculating the spin-orbit mixing angle. The results show that Ba has a mixing angle that is five times that of Sr, while the factor for Sr and Ca is only 2 [29]. In fact, the predictions of an MQDT model based on the assumption of pure LS-coupled Sr $5snd$ "close coupling" eigenchannel agree well with experiments [29,30]. In other words, Sr is the heaviest alkaline-earth atom whose characteristics can be correctly reproduced without introducing spin-orbit coupling. Based on the facts mentioned above, it is reasonable to make an approximation in which the Sr atom is treated in the same way as Ca. By analogy with Ca [31], we decided to treat $^1D_2$ and D_2 Rydberg series separately, spin-orbit interaction being disregarded. As far as the fitting process is concerned, this affects only a limited number of levels; hence the calculated energies can be compared with the experimental ones. Besides, it will be very interesting to see to what extent this approximation may affect the lifetime prediction.

The initial step in an MQDT analysis is to identify the relevant channels, which proceeds as follows: The two principal channels are the $^{1,3}D_2$ Rydberg series of the $5snd$ configuration, which converge to the $5s$ ionization limit. The perturbing channels are those associated with the Rydberg series of doubly excited configurations converging to higher ionization limits. Obviously only the lowest members of those series converging to the lowest excited states of ions are important.

A. MQDT treatments

1. Singlet term

Both R-matrix [30] and multiconfiguration Hartree-Fock calculations [32,33] have demonstrated that the $5snd$-$4dnd$ mixing is stronger than the $5snd$-$5pnp$ mixing below the Sr^+5s limit. Furthermore, the R-matrix calculation suggests that the $5p^2\ ^1D_2$ perturber is above the Sr^+5s limit ($5p^2\ ^1D_2$ is at 46 200 cm^{-1}), and that the level at 36 361 cm^{-1} should be labeled as $4d^2$ instead [30]. For all the reasons above, a three-channel model ($5snd$, $4dns$, and $4dnd$) is chosen here to analyze the $^1D_2$ spectrum, which makes the situation clear: while the lowest members of the $5snd\ ^1D_2$ series are perturbed by the $4d^2\ ^1D_2$ state, higher members of the $J=2$ series are affected by the $4dns$ state leading to a singlet-triplet mixing.

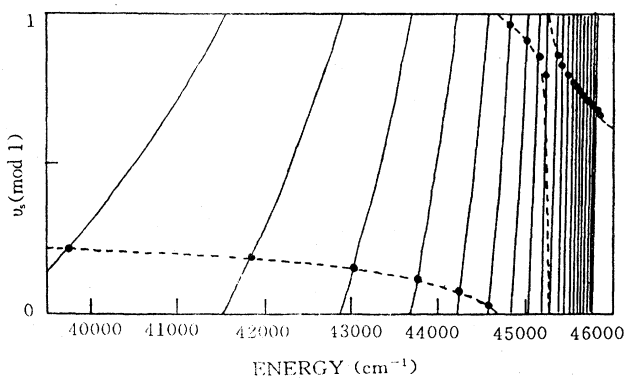

FIG. 4. Plot of the effective quantum number ν_{5s} (mod 1) versus the term energy. The curves are calculated from Eq. (1) (solid line) and Eq. (2) (dashed line), respectively, whose crossings give the calculated energy levels, to be compared with the experiment data (closed circle) of the $5snd\ ^1D_2$ states.

For the sake of convenience, the $5snd$, $4dns$, and $4dnd$ channels are labeled as channels 1, 2, and 3, respectively, which only introduces two limits: $I_1=I_s$ and $I_2=I_3=I_d$, the average of the spin-orbit split $4d^+_{3/2}$ and $4d^+_{5/2}$ limits. In the analysis we have to first determine values for $U_{i\alpha}$ and μ_α such that the calculated ν_i agree with the experimental values. In practice the U matrix is written as the product of three matrices, corresponding to rotations through three angles. In other words, there exist a total of six free parameters, three determining the U matrix and others the μ_α values.

Note that the $5s5d\ ^1D_2$ state is excluded from the fit, since the lowest member of a Rydberg series is not suitable for MQDT analysis. Thus an energy dependence of the parameters need not be considered. The best fit is shown in Fig. 4 (dashed line) and yields

$$U=\begin{bmatrix} 0.905 & 0.103 & -0.414 \\ -0.106 & 0.994 & 0.015 \\ 0.413 & 0.030 & 0.910 \end{bmatrix} \tag{10}$$

and

$$\mu_1=0.777, \quad \mu_2=0.332, \quad \mu_3=0.289. \tag{11}$$

The two classes of curves plotted in Fig. 4 are calculated from Eq. (1) (solid line) and Eq. (2) (dashed line), respectively. The intersections of the two curves are the simultaneous solutions of the two equations, and thus represent the calculated energy levels, to be compared with the experimen-

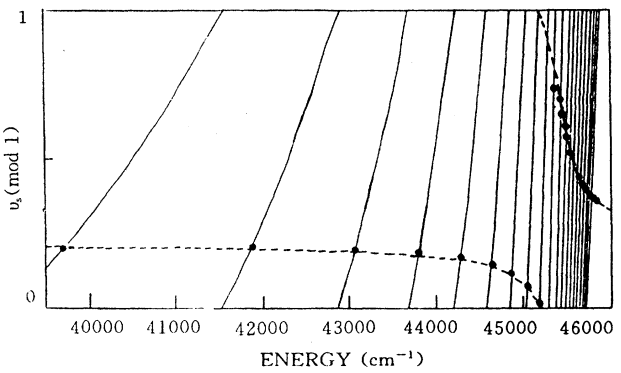

FIG. 5. Plot of the effective quantum number ν_{5s} (mod 1) versus the term energy. The caption of Fig. 4 applies, except this plot is for $5snd\ ^3D_2$ states.

tal data (closed circles). The comparison between the theory and experiments (the present and the previous ones [1,2,18]) is provided in Table I. It is important to realize that one of the advantages of the MQDT is that rather than treating one state at a time, the level energies of the whole series are solved as a single problem. To fulfill this realization, the calculated energies with higher n values ($n>50$) are presented, which is in harmony with the results of the high-resolution measurement [2]. The deviation from the present measurement is in reasonable agreement with the experimental error (~ 0.2 cm^{-1}). The largest deviations occur around the $5snd$ states with $n=10$–15. This is expected due to the strongest singlet-triplet mixing in the region, which is neglected in this treatment. In addition, ten unmeasured levels are predicted and shown in Table I.

2. Triplet term

A two-channel model ($5snd$, $4dns$) has been chosen to describe the perturbation of the high-lying $5snd\ ^3D_2$ level by the $4d6s\ ^3D_2$ perturber. If we label the $5snd$ and $4dns$ channels as channels 1 and 2, respectively, then $I_1=I_s$ and $I_2=I_d$, the average of $4d^+_{3/2}$ and $4d^+_{5/2}$ limits. Note that the $5s5d$, $5s6d$ states have been excluded from the fit. The similar procedure to the $^1D_2$ spectrum is performed to give the best fit, shown in Fig. 5, and MQDT parameters as follows:

$$U_{11}=U_{22}=\cos\theta, \quad U_{12}=-U_{21}=\sin\theta, \tag{12}$$

with

$$\mu_1=0.785, \quad \mu_2=0.313, \quad \theta=0.227. \tag{13}$$

The description of Fig. 5 is similar to that of Fig. 4. In Table II, the calculated energies ($n\leq 40$) together with those from the present experiment and others [1,18] are listed. Additional calculated energies, which are unmeasured, are also tabulated. Generally speaking, the model reproduces experimental data correctly with slight disagreement for n ranging from 10 to 18 as expected, since the information on the singlet-triplet mixing is lost in the current treatment. A five-channel MQDT treatment of the Sr $5snd$ series [1] is helpful in providing the above information. By treating the singlet and triplet terms simultaneously one is able to reproduce the spectrum in the vicinity of the perturber accurately. A comparison between the present MQDT results and those of Ref. [1] is provided in Tables I and II. In most cases, the two MQDT models agree well. In the region near a perturber Ref. [1] shows better agreement, as expected. The calculated energies for n up to 85 are available; they remain to be tested by new experiments and are not presented here.

Turning now to wave functions, as we know, once the MQDT parameters of the $^{1,3}D_2$ terms are determined, the wave function is known for all energies. This can be done using Eqs. (5) and (6). The admixtures of the $5snd\ ^{1,3}D_2$ configurations give the interpretation of the $4d6s\ ^{1,3}D_2$ perturbation. Our results of A_i^2 confirmed that the $4d6s\ ^{1,3}D_2$ level spread out over many $5snd$ levels, and no state deserves the label $4d6s\ ^1D_2$ or $4d6s\ ^3D_2$. However, for the singlet term, a maximum admixture of 4.8% in the $5s11d$ level is found, to be compared with the 4.6% [1] and 3.5% [30] in the previous studies. For the triplet state, the calculation shows that the maximum admixture, per state, occurs in the $5s17\ ^3D_2$ level with a value of 11%, consistent with the previous values of 10% [1] and 7.8% [30], respectively.

In both cases, the information on the lowest levels is inaccurate owing to the exclusions of the lowest levels in both fits. Also, the calculations show that the $4d6s\ ^{1,3}D$ states mainly affect a limited numer of states of the $5snd$ series, while for $n\leq 10$ and $n\geq 25$ either the $^1D_2$ or $^3D_2$ state is virtually a "pure" state.

B. Lifetime

In Sr, strong perturbation in seuqences of highly excited states occurs due to the interaction with low-lying valence states of series of the same parity, converging towards a higher series limit. Configuration mixing not only affects the level positions and wave functions but is also reflected in radiative lifetime. Lifetime measurements in the $5snd$ series of Sr are able to give us an insight into atomic wave functions and yield the possibility of checking theoretical calculations.

1. $^1D_2$ term

Based on the calcualted mixng coefficients $A_i^{(n)}$ for the $5snd\ ^1D_2$ Rydberg series, we are able to evaluate lifetimes of Sr in the perturbed $5snd\ ^1D_2$ ($n=6$–25) series. This is carried out through the least-squares-fitting procedure using the lifetime data available. In our case, 14 experimental lifetimes are used to determine seven parameters, which is not an ideal situation for fitting purposes, but should be acceptable. The best fit is shown in Fig. 6 and yields the parameters $k=-1.63$ and Γ_{ij}. The values of Γ_{ij} are listed in Table III. Figure 6 shows the variations in the lifetime trends, as well as pronounced deviation from the simple scaling law $\tau\sim(n^*)^3$. $n^*(=\nu_{5s})$ is the effective principal quantum number. The exact values for $n=6$–25 states are given in Table IV together with the experimental data. Several unmeasured lifetimes are also predicted. The lifetimes for $n=6$–9 states, calculated from the Hartree-Slater core approximaton (HSCA) [8] are also listed for comparison.

As shown in Table IV, most of the calculated lifetimes agree well with experimental ones within their uncertainties

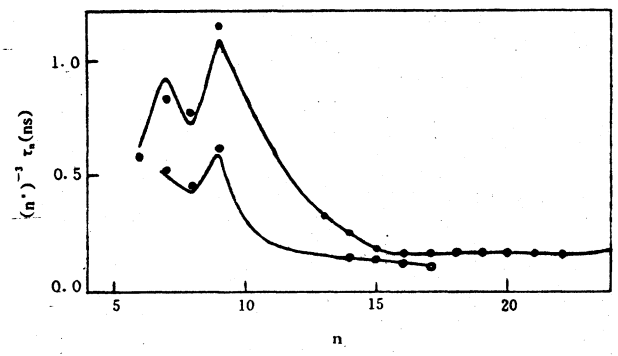

FIG. 6. Lifetimes of the $5snd\ ^{1,3}D_2$ Rydberg states. The experimental data are indicated by the closed circles ($^1D_2$ term) and open circles ($^3D_2$ term), respectively. They are taken from Refs. [9,10,34]. The curves are obtained by the two separate fits. For the $^1D_2$ term the parameters yielded are shwon in Table III; the parameters for the $^3D_2$ term are shown in the text. In both cases, the irregularities in lifetimes with $(n^*)^3$ are demonstrated.

listed in parentheses; the shortenings in the lifetime values around $n=15$ are also correctly reproduced. However, the calculated lifetimes for the two lowest states are too long. This may be attributed to the inaccurate wave functions for those states caused by the ignorance of the lowest member of the $5snd\ ^1D_2$ series in our MQDT treatment. Referring to Table I, note that the energies of $n=6$ and 7 states are predicted by the theory reasonably well. This indicates that the same model does not necessarily predict the different observables equally well. In other words, lifetime is a more stringent test than energy to the influence of a $4d^2\ ^1D_2$ perturber, which is highly localized in the lowest states of the $5snd\ ^1D_2$ Rydberg series.

2. $^3D_2$ term

The lifetimes of Sr $5snd\ ^3D_2$ Rydberg states have been calculated using the mixing coefficinets $A_i^{(n)}$ obtained. Applying a similar procedure, we achieve the best fit, shown in Fig. 6, with the following parameters: $k=-1.534$, $\Gamma_{11}=21.918$, $\Gamma_{21}=-3.131$, and $\Gamma_{22}=0.586$. The units for Γ_{ij} are $10^9\ s^{-1}$. They are determined by fiting experimental data of lifetimes. Since the number of lifetime data (seven) is small, fitting them to above four parmeters is not an ideal case, either. For this reason we only give several predictions for unmeasured states in Table V, which lists the calculated and experimental values of lifetime. Again the calculated values agree well with those of experiment within their experimental uncertainties. Note that unlike the $^1D_2$ term, agreement between theory and experiment is satisfactory for the lower n states. In addition, several theoretical lifetimes from the HSCA calculation [8] are also tabulated for reference.

TABLE III. Values of parameters $\Gamma_{ij}(=\Gamma_{ji})$; units are $10^9\ s^{-1}$.

i \ j	1	2	3
1	5.7027		
2	8.0612	−0.5998	
3	−10.4920	−2.5571	4.6345

TABLE IV. Measured [10] and calculated lifetimes of Sr $5snd\ ^1D_2$ Rydberg States. Lifetimes for $n=6$–9 states are from Ref. [9], and the errors are shown in parentheses.

n	Expt. (ns)	Theory (ns)	HSCA [8]
6	42.6(2.2)	47.0	49.3
7	114.5(4)	131.5	90
8	182(16)	162.7	149
9	413(46)	387.4	243
10		442.0	
11		440.6	
12		438.6	
13	410(20)	429.0	
14	408(12)	404.2	
15	340(10)	336.3	
16	365(15)	380.7	
17	517(16)	503.6	
18	640(16)	626.3	
19	738(37)	771.2	
20	866(40)	904.2	
21	1023(51)	1008.7	
22	1190(60)	1153.3	
23		1378.2	
24		1750.4	
25		1940.3	

Note that in both cases of singlet and triplet the n^{*3} scalng was tried, which does not work in general, although the simple scaling law works better in the range away from a perturber. In order to avoid performing separate fits for the same term and to give it a unified treatment so that the MQDT wave function can be tested, we have applied the formalism described in Sec. III and have found that in a fit the number of parameters that are necessary to describe sharp variations of lifetimes was increased rapidly.

To summarize, for either the triplet or singlet term, the MQDT models do not provide accurate values for energies around $n=15$ (shown in Tables I and II) but give acceptable values for lifetimes in the same region. This infers that the lifetime may be less sensitive to the singlet-triplet mixing

TABLE V. Measured and calculated lifetimes of Sr $5sns\ ^3D_2$ Rydberg States. Lifetimes for $n=14$–17 and $n=7$–9 are from Refs. [10] and [34], respectively, whose errors are shown in parentheses.

n	Expt. (ns)	Theory (ns)	HSCA [8]
7	74(4.8)	69.2	62.8
8	108(5)	96.7	99
9	232(8)	218.0	143
10		153.3	
11		141.6	
12		169.8	
13		185.4	
13		185.4	
14	247(8)	246.4	
15	282(11)	283.9	
16	286(9)	279.7	
17	319(15)	323.2	

induced by the $4d6s\ ^{1,3}D_2$ perturbers. The less sensitivity to the singlet-triplet mixing has been found in Ba $6snd\ ^{1,3}D_2$ sequences previously [35]. Great deviations from experimental g_J factors were found, although the same model predicted lifetimes very well. It seems that lifetime data only test a part of the MQDT wave functions, that is the perturber character. In other words, the lifetime values are mainly sensitive to the total admixture coefficient of doubly excited configurations. However, since lifetimes are dominated by the outer parts of the wave functions, agreement between the theory and experiment suggests that the outer parts of the wave functions that are derived from experimental energies are accurate.

V. CONCLUSION

We have measured the energy levels of Sr $5snd\ ^{1,3}D_2$ sequences with $n=9-50$ ($^1D_2$ term) and $n=9-37$ ($^3D_2$ term), respectively. We have calculated the energy levels using an empirical MQDT formalism. The $^1D_2$ and $^3D_2$ Rydberg series are treated with two separate models. Overall agreement between the theory and experiment on energy is achieved. The MQDT wave functions derived from energy are tested by evaluating the radiative lifetimes of the same series, which agree well with the measured lifetime data with exceptions for the lowest members of the series.

The same set of MQDT parameters predicts energy better than lifetime for the low-lying states, indicating that lifetime is more sensitive than energy to the influence of the $4d^2$ perturbers. The situation is different for the singlet-triplet mixing, which affects the energy more than lifetime. In the region where the $4d6s$ perturbers play a great role, lifetime may be reproduced correctly without taking the singlet-triplet mixing into account.

ACKNOWLEDGMENTS

This work was supported by the National Natural Science Foundation of China, the State Commission of Education of China, and The Science Foundation of Zhejiang University. The author acknowledges X. A. Zhao and Y. F. Xu for their contributions to the experiment.

[1] P. Esherick, Phys. Rev. A **15**, 1920 (1977).
[2] R. Beigang *et al.*, Opt. Commun. **42**, 19 (1982).
[3] J. R. Rubbmark and S. A. Borgström, Phys. Scr. **18**, 196 (1978).
[4] R. Beigang and D. Schmidt, Physica Scr. **27**, 172 (1983).
[5] E. Y. Xu *et al.*, Phys. Rev. A **33**, 2401 (1986).
[6] J. J. Wynne, J. A. Armstrong, and P. Esherick, Phys. Rev. Lett. **39**, 1520 (1977).
[7] R. Beigang, E. Matthias, and A. Timmermann, Phys. Rev. Lett. **47**, 326 (1981).
[8] H. G. C. Werij *et al.*, Phys. Rev. A **46**, 1248 (1992).
[9] W. Gornik, Z. Phys. A **283**, 231 (1977).
[10] P. Grafström *et al.*, Phys. Rev. A **27**, 947 (1983).
[11] P. T. Greenland, Contemp. Phys. **31**, 405 (1990).
[12] J. Boker, R. R. Freeman, and W. E. Cooke, Phys. Rev. Lett. **48**, 1242 (1982).
[13] K. LaGattuta and Y. Hahn, Phys. Rev. Lett. **51**, 558 (1983).
[14] S. E. Harris, Phys. Rev. Lett. **62**, 1033 (1989).
[15] W. E. Cooke *et al.*, Phys. Rev. Lett. **40**, 178 (1978).
[16] C. J. Dai, G. W. Schinn, and T. F. Gallagher, Phy. Rev. A **42**, 223 (1990).
[17] E. Y. Xu *et al.*, Phys. Rev. A **35**, 1138 (1987).
[18] C. E. Moore, *Atomic Energy Levels*, Nat'l. Bur. Stand. U.S. Circ. No. 467 (U.S. GPO, Washington, DC, 1952), Vol. 2.
[19] C. J. Dai, S. M. Jaffe, and T. F. Gallagher, J. Opt. Soc. Am. B **6**, 1486 (1989).
[20] G. W. Schinn, C. J. Dai, and T. F. Gallagher, Phys. Rev. A **43**, 2316 (1991).
[21] R. R. Jones, C. J. Dai, and T. F. Gallagher, Phys. Rev. A **41**, 316 (1990).
[22] M. D. Lindsay *et al.*, Phys. Rev. A **45**, 231 (1992).
[23] M. D. Lindsay *et al.*, Phys. Rev. A **46**, 3789 (1992).
[24] Y. Zhu, E. Y. Xu, and T. F. Gallagher, Phys. Rev. A **36**, 3751 (1987).
[25] M. J. Seaton, Proc. Phys. Soc. **88**, 801 (1966); Rep. Prog. Phys. **46**, 167 (1983).
[26] C. M. Lee and K. T. Lu, Phys. Rev. A **8**, 1241 (1973); W. E. Cooke and C. L. Cromer, *ibid.* **32**, 2752 (1985); A. Giusti-Suzor and U. Fano, J. Phys. B **17**, 215 (1984).
[27] M. Aymar *et al.*, J. Phys. B **14**, 4489 (1981).
[28] X. W. Liu and Z. W. Wang, Phys. Rev. A **40**, 1838 (1989).
[29] M. Aymar, Phys. Rep. **110**, 163 (1984).
[30] M. Aymar, E. Luc-Koenig, and S. Watanabe, J. Phys. B **20**, 4325 (1987).
[31] J. A. Armstrong, P. Esherick, and J. J. Wynne, Phys. Rev. A **15**, 180 (1977).
[32] A. Aspect *et al.*, J. Phys. B **17**, 1761 (1984).
[33] N. Vaeck, M. Godefroid, and J. E. Hansen, Phys. Rev. A **38**, 2830 (1988).
[34] A. L. Osherovich *et al.*, Opt. Spectrosc. (USSR) **46**, 134 (1979).
[35] P. Grafström *et al.*, Z. Phys. A **308**, 95 (1982).